Journal of Nuclear Medicine, published on July 16, 2021 as doi:10.2967/jnumed.121.261939

Striatal acetylcholine-dopamine imbalance in Parkinson's disease: *in vivo* neuroimaging study with dual-tracer PET and dopaminergic PET-informed correlational tractography

Short running title: Acetylcholine-dopamine imbalance in PD.

Carlos A. Sanchez-Catasus[1-,3], Nicolaas I. Bohnen[1, 3-5], Nicholas D'Cruz[6], Martijn L.T.M. Müller[1,3]

[1]Department of Radiology, Division of Nuclear Medicine, University of Michigan Health System, Ann Arbor, MI, USA.

[2]Department of Nuclear Medicine and Molecular Imaging, University Medical Center Groningen, Groningen, Netherlands.

[3]Morris K. Udall Center of Excellence for Parkinson's Disease Research, University of Michigan, Ann Arbor, MI, USA.

[4]Department of Neurology, University of Michigan Health System, Ann Arbor, MI, USA.

[5]Neurology Service and GRECC, Veterans Administration Ann Arbor Healthcare System, Ann Arbor, MI, USA.

[6]Department of Rehabilitation Sciences, KU Leuven, Leuven, Belgium.

Corresponding author: Martijn L.T.M. Müller; Critical Path Institute, E-mail: mmuller@c-path.org

First author: Carlos A. Sanchez-Catasus ; casanchezcatasus@gmail.com

ABSTRACT

Previous studies of animal models of Parkinson's disease (PD) suggest an imbalance between striatal acetylcholine (ACh) and dopamine (DA), although other studies have questioned this. To our knowledge, there are no previous in vivo neuroimaging studies examining striatal ACh-DA imbalance in PD patients. Using cholinergic and dopaminergic PET (^{18}F-FEOBV and ^{11}C-DTBZ, respectively) and correlational tractography, our aim was to investigate the ACh-DA interaction at two levels of dopaminergic loss in PD subjects: integrity loss of the nigrostriatal dopaminergic white matter tract; and loss at the presynaptic-terminal level. **Methods:** The study involved 45 subjects with mild to moderate PD (36 men, 9 women; mean age, 66.3 ± 6.3 years, disease duration, 5.8 ± 3.6; Hoehn and Yahr stage, 2.2 ± 0.6) and 15 control subjects (9 men, 6 women; mean age, 69.1 ± 8.6 years). PET imaging was performed using standard protocols. We first estimated the integrity of the dopaminergic nigrostriatal white matter tracts in PD subjects by incorporating molecular information from striatal ^{11}C-DTBZ PET into the fiber tracking process using correlational tractography (based on quantitative anisotropy, QA; a measure of tract integrity). Subsequently, we used voxel-based correlation to test the association of the mean QA of the nigrostriatal tract of each cerebral hemisphere with striatal ^{18}F-FEOBV distribution volume ratio (DVR) in PD subjects. The same analysis was performed for ^{11}C-DTBZ DVR in 12 striatal subregions (presynaptic-terminal level). **Results:** Unlike ^{11}C-DTBZ DVR in striatal subregions, the mean QA of the nigrostriatal tract of the most affected (MA) hemisphere showed a negative correlation with a striatal cluster of ^{18}F-FEOBV DVR in PD subjects (*p corrected= 0.039*). We also found that the mean ^{18}F-FEOBV DVR within this cluster was higher in the PD group compared to the control group (*p = 0.01*). Cross-validation analyses confirmed these findings. We also found an increase of bradykinesia ratings associated with increased ACh-DA

imbalance in the MA hemisphere (*r=0.41, p= 0.006*). **Conclusion:** Our results provide evidence for the existence of striatal ACh-DA imbalance in early PD and may provide an avenue for testing in vivo effects of therapeutic strategies aimed at restoring striatal ACh-DA imbalance in PD.

Key words: Parkinson disease, acetylcholine-dopamine imbalance, dopaminergic nigrostriatal connectivity, ^{18}F-FEOBV PET, ^{11}C-DTBZ PET.

INTRODUCTION

Striatal cholinergic interneurons are the main source of cholinergic innervation in the striatum (*1*,*2*). Although these interneurons represent a small percentage of all striatal neurons, they are distributed throughout the striatum and their presynaptic terminals overlap with dopaminergic axonal projections originating in the substantia nigra pars compacta (*2*). A prevailing view is that the acetylcholine (ACh) and dopamine (DA) signaling systems must be in dynamic balance in the striatum for optimal movement control (*3*,*4*).

Parkinson's disease (PD) is a neurodegenerative movement disorder characterized by nigrostriatal dopaminergic losses (*5*,*6*). These losses may result in a striatal ACh-DA imbalance (*3*), at least in the early disease stages. Although several animal model studies support this concept (for recent reviews see *7-9*), other studies have questioned the ACh-DA imbalance model (*10-12*). For example, Herrera-Marschitz et al. found that striatal acetylcholine levels were not modified by unilateral dopaminergic deafferentation in a rat model (*10*). In a subsequent study, they suggested that striatal dopamine and acetylcholine release is modulated by independent mechanisms (*11*). A more recent study suggested that striatal dopamine deficiency decreased acetylcholine production and inhibited normal striatal cholinergic interneuron spike timing in Parkinsonian mice (*12*). They also found that acetylcholine decreased to a lesser extent than dopamine resulting in an increased ACh/DA ratio (*12*) suggestive of the ACh-DA imbalance in PD.

To the best of our knowledge, there are no prior *in vivo* studies in humans with PD that examine changes in striatal cholinergic interneuron activity in response to nigrostriatal dopaminergic

losses. A better understanding of striatal dopaminergic and cholinergic systems interaction may have implications for the development of new therapeutic strategies in PD.

^{18}F-fluoroethoxybenzovesamicol (^{18}F-FEOBV) is a PET radioligand that selectively binds to the vesicular acetylcholine transporter and allows for binding quantification in brain regions with high presynaptic cholinergic activity, such as the striatum (*13*). ^{11}C dihydrotetrabenazine (^{11}C-DTBZ) selectively binds to the vesicular monoamine transporter type 2 and is useful as a marker of the nigrostriatal dopaminergic presynaptic-terminal due to the high specificity in the striatum (*14*). However, like other PET dopaminergic presynaptic markers, ^{11}C-DTBZ may be influenced by pharmacological compensation or regulation (*15-17*). These processes might obscure the striatal DA-ACh interaction at the presynaptic-terminal level, therefore more robust approaches may be required to capture dopaminergic transmission.

We recently introduced a methodology to estimate dopaminergic nigrostriatal white matter tract integrity (i.e., dopaminergic nigrostriatal connectivity) in subjects with early PD (*18*). This methodology integrates striatal ^{11}C-DTBZ PET information into the fiber tracking process using diffusion magnetic resonance imaging (dMRI)-based correlational tractography. Tract integrity is measured as the mean quantitative anisotropy (QA) across the estimated tract. QA measures the density of anisotropic diffusion water (*19*) and provides a more reliable integrity metric compared to standard diffusion measures (*18, 20,21*). Furthermore, the dopaminergic nigrostriatal white matter tract should be less influenced by compensatory mechanisms compared to the presynaptic-terminal level.

Using in vivo cholinergic and dopaminergic PET and dopaminergic PET-informed correlational tractography, our aim was to examine the striatal ACh-DA imbalance hypothesis in patients with

early PD while considering the integrity loss of the nigrostriatal dopaminergic pathway at two levels: dopaminergic nigrostriatal connectivity (i.e., loss of mean QA of the nigrostriatal tract); and the presynaptic-terminal level (i.e., loss of striatal ^{11}C-DTBZ binding). We also examined differences in striatal cholinergic binding between PD subjects and healthy controls.

MATERIALS AND METHODS

Subjects

The study included forty-five subjects with mild to moderate PD (36 men and 9 women; mean age 66.3 ± 6.3 years), of whom 30 subjects were previously reported (*18*). The study also included fifteen age- and gender-matched healthy control subjects (9 men and 6 women; mean age 69.1 ± 8.6 years) with available cholinergic ^{18}F-FEOBV PET.

Similar to our previous report (*18*), PD subjects were selected based on three criteria: 1) only subjects with mild to moderate PD (Hoehn and Yahr (HY) stage ≤ 3) were included to avoid a floor effect associated with severe nigrostriatal dopaminergic denervation in more advanced stages; 2) high-quality dMRI reconstruction; and 3) a time interval between clinical examinations and neuroimaging assessments of 2 months or less to ensure no significant clinical interval changes. Table 1 summarizes the main demographic and clinical characteristics of all participants.

All patients met the UK Parkinson's Disease Society Brain Bank clinical diagnostic criteria for PD (*22*) and showed the typical pattern of striatal dopaminergic denervation on ^{11}C-DTBZ PET congruent with this diagnosis (*14*). The Movement Disorder Society-revised Unified Parkinson's Disease Rating Scale (MDS-UPDRS) examination (*23*), the HY scale (*24*), and the Montreal

Cognitive Assessment (MoCA) test (*25*) were performed in PD subjects for clinical assessments. The motor examination was performed in the dopaminergic medication "OFF" state, except for two de-novo patients. No subjects were treated with anti-cholinergic or cholinesterase inhibitor drugs. In 29 patients, motor symptoms were predominantly on the right side of the body while in the other 16 patients were predominantly on the left side.

The study was approved by the Institutional Review Boards of the University of Michigan School of Medicine and Veterans Affairs Ann Arbor Healthcare System. Written informed consent was obtained from all subjects prior to any research procedures.

Imaging Procedures

We realigned (right to left) image data of the 16 patients with a left predominance of clinical symptoms in order to create a uniform sample given the asymmetry in early PD for the typical motor symptoms and striatal ^{11}C-DTBZ (*14*). Thus, the left hemisphere represented the clinically "most affected" (MA) hemisphere in all patients, and the right hemisphere the clinically "least affected" (LA).

PET Imaging. All subjects underwent both PET scans during the same visit, except for control subjects in whom dopaminergic PET was not performed. Dynamic PET imaging was performed in 3D mode using an ECAT Exact HR tomograph (Siemens Molecular Imaging, Inc.). Preprocessing of both PET data can be found in detail elsewhere (*26,27*). ^{11}C-DTBZ (555 MBq) and ^{18}F-FEOBV (256 MBq) radioligands were prepared as previously described and injected following standard routines (*28,29*). Dopaminergic PET was performed in the dopaminergic "OFF" state, while cholinergic PET was performed in the "ON" state in PD subjects.

For both PET tracers, dynamic frames were spatially co-registered within-subject with a rigid body transformation to reduce the motion effect during the imaging session (*30*). Motion-corrected PET frames were spatially co-registered to high-resolution MRI using SPM12 software (Wellcome Trust Centre for Neuroimaging, London, UK, https://www.fil.ion.ucl.ac.uk/spm). Distribution volume ratio (DVR) images were then calculated for the two PET tracers following previously reported methodologies (*31*,*32*).

For MRI co-registered ^{11}C-DTBZ DVR images, we manually traced the volumes corresponding to six striatal subregions in each brain hemisphere on the MRI scan following a methodology described previously (*33*). The striatal subregions included the anteroventral striatum, middle caudate, caudate head, ventral putamen, anterior putamen, and posterior putamen. These striatal subregions encompass the typical ventral to dorsal and anterior to posterior gradient of striatal dopaminergic denervation in early PD (*33*) and were used as striatal dopaminergic variables of interest at the presynaptic-terminal level in the voxel-based correlation analysis with striatal ^{18}F-FEOBV DVR. Supplementary Figure 1 shows the histograms, mean (± standard deviation), and median (range) of ^{11}C-DTBZ DVR of these subregions. The analysis was also carried out with the whole striatum as a variable of interest.

For voxel-based correlation analysis, ^{18}F-FEOBV DVR images were spatially standardized to the Montreal Neurological Institute (MNI) space based on the Diffeomorphic Anatomical Registration Through Exponentiated Lie Algebra (DARTEL) procedure (SPM12). DARTEL transformations were estimated based on T1-weighted MRI and subsequently applied to PET images co-registered with MRI. ^{18}F-FEOBV DVR images of control subjects were transformed in the same way to perform a voxel-based group comparison. Spatially normalized ^{18}F-FEOBV DVR images were smoothed with the SPM12 default Gaussian isotropic kernel of 8 mm at full

width half maximum to reduce the anatomical variability between individual brains and to enhance the signal-to-noise ratio.

MRI Imaging. All subjects underwent high-resolution structural brain MRI (T1-weighted) for anatomical co-registration with the corresponding PET scans as described above. MRI was performed on a 3T Philips Achieva system (Philips). A detailed description of structural brain MRI acquisition parameters can be found elsewhere (*26*).

During the same visit, dMRI was obtained for dopaminergic PET-informed correlational tractography. The acquisition parameters and preprocessing of the MRI images have been described in detail previously (18). Quality control of the preprocessed dMRI image data was performed using DSI-studio toolbox (http://dsi-studio.labsolver.org). The neighboring correlation was high and similar across all dMRI volumes (0.88 ± 0.02), indicating a very good quality of preprocessed dMRI data relative to motion artifacts and signal-to-noise ratio.

Dopaminergic PET-informed Correlational Tractography. Correlational tractography was performed as previously (*18*) in a larger sample of PD participants. In brief, dMRI preprocessed data in the PD group were reconstructed in the MNI space using q-space diffeomorphic reconstruction (*34*) implemented in DSI Studio toolbox. Our correlational tractography-based approach first constructs a group-based "tract template" in each brain hemisphere by tracking QA in white matter fibers that correlate with ^{11}C-DTBZ DVR corresponding to anteroventral striatum to optimally guide tract reconstruction with “dopaminergic” specificity” (*18*). The procedure uses a deterministic fiber tracking (*35*), with the substantia nigra as the seed region and the whole striatum as the terminating region corresponding to each brain hemisphere. In a

second step, the mean QA extracted from each subject across the template (from each hemisphere) was used as a measure of the whole tract integrity at the individual level.

The individual mean QA values of each PD subject in each hemisphere and the striatal subregions described above and the whole striatum were used as dopaminergic variables of interest the voxel-based correlation analysis with striatal ^{18}F-FEOBV DVR.

Statistical Analysis

Voxel-based correlation analysis was performed using SPM12 to test the association of mean QA of the dopaminergic nigrostriatal tract or striatal subregional presynaptic-terminal ^{11}C-DTBZ DVR (and the whole striatum) of each hemisphere with striatal ^{18}F-FEOBV DVR in PD subjects. An explicit bilateral mask was used to exclude non-striatal voxels. Age and sex were modeled as standard nuisance covariates. Positive and negative correlations were tested. The results of this analysis were then used to create a volume of interest (VOI), based on significant clusters, to evaluate Pearson correlation of the VOI mean values of ^{18}F-FEOBV DVR with the corresponding dopaminergic variables of interest, and for comparison between groups (PD versus control) within that VOI using Student's t-test for independent samples.

In a second analysis, levodopa equivalent dose, duration, and the stage of the disease (defined as a binary variable according to the HY scale: mild = 0 for HY $\leq$ 2; moderate= 1 for 2 < HY $\leq$ 3) were considered as additional nuisance covariates to test their possible confounding effects on the first voxel-based correlation analysis.

Since the presence of outliers in the data can affect the correlation analysis, we repeated voxel-based correlation analysis for dopaminergic variables of interest that showed potential outliers.

For outlier detection, we used the Grubbs test. In the event that a variable was significant for the Grubbs test and did not have a normal distribution (significant Shapiro-Wilk test, see Supplementary Figure 1), we also used the interquartile rule to find outliers as follows: First, calculation of the interquartile range (IQR) of the data of each subregion; Second, calculation of the lower boundary by subtraction 1.5 x (IQR) from the first quartile; And third, calculation of the upper boundary by adding 1.5 x (IQR) to the third quartile. Any value outside the upper and lower boundaries was considered a potential outlier.

Additionally, a voxel-based group comparison was performed between the control and PD groups for striatal ^{18}F-FEOBV DVR, controlling for age and sex.

In all SPM analyses, we used a threshold of $p = 0.001$ (uncorrected) at voxel-level and $p = 0.05$ corrected for multiple comparisons at cluster-level by using the family-wise error (FWE) approach.

Cross-Validation. To assess the generalizability of our main findings, cross-validation was performed using the leave-one-out (LOO) methodology. Since the mean QA of the dopaminergic nigrostriatal tract in the MA hemisphere (Figure 1.A) was the only dopaminergic variable of interest that showed a significant correlation with the striatal ^{18}F-FEOBV DVR, the cross-validation was applied to this model (MA-tract model) and to the VOI model derived from the voxel-based correlation analysis (Figure 1.B).

MA-tract model: In this model, the training set was defined as the mean QA extracted in each PD subject from the group-based "tract template" in the MA hemisphere. To get the validation element of a single PD subject, we constructed a new tract template but leaving that specific PD

subject out. This new tract template was used to extract the mean QA from that PD subject (mean QA-LOO). This process was repeated for each of the 45 PD subjects.

VOI model: In this model, the training set was defined as the mean ^{18}F-FEOBV DVR value of each PD subject within the VOI based on SPM voxel-based correlation analysis (mean VOI), as described above. To get the validation element of a single PD subject, we repeated the SPM analysis but leaving that specific PD subject out. The new VOI (the significant cluster) was used to extract the mean ^{18}F-FEOBV DVR value from that PD subject (mean VOI-LOO). This process was repeated for each of the 45 PD subjects.

To summarize the error between the predicted and observed values for the two models, the normalized root-mean-square error was used. Pearson correlation was then used to assess the association of mean QA- LOO and mean VOI-LOO.

Clinical Correlate. To assess the clinical relevance of our main findings, we examined whether the cardinal motor features (sub-scores of bradykinesia, tremor, rigidity, and postural instability and gait difficulties) and cognitive function (Montreal Cognitive Assessment, MoCA score) of PD subjects, correlated with the following ratio in the MA hemisphere (a proxy measure of ACh-DA imbalance in this hemisphere):

$$\frac{\text{mean } 18\text{F} - \text{FEOBV DVR within the putaminal SPM} - \text{based VOI}}{\text{mean QA of the nigrostriatal white matter MA tract}}$$

To show robustness of the dopaminergic PET-informed correlational tractography, we also repeated previous analyses in this larger sample of PD participants.

Non-voxel-based statistical analyses were carried out using STATISTICA software (Stat Soft, Inc., version 8.0). The significance level was set at $p < 0.05$. For the correlation tests, we used Pearson's correlation for normally distributed variables based on the Shapiro–Wilk test (mean QA (LA and MA), mean QA-LOO (MA), mean VOI, mean VOI-LOO, imbalance proxy, imbalance proxy – LOO, bradykinesia and tremor sub-scores) otherwise we used Spearman's correlation. For significant results, we also computed 95 % percentile bootstrap confident intervals (CI).

RESULTS

Association Between the Integrity of Dopaminergic Nigrostriatal White Matter Tracts and Striatal Cholinergic Binding in PD Subjects

The mean QA of the MA-tract (Figure 1. A) showed a negative correlation with striatal ^{18}F-FEOBV DVR (Figure 1. B), which comprised a cluster in the posterior putamen of the MA hemisphere; p corrected at the cluster level = 0.039; cluster size= 226 voxels; MNI coordinates (x, y, z) of the maximum peak= -27, -9, 11; t value at the peak-level= 4.05. Figure 1.C shows the negative correlation found between mean QA and mean ^{18}F-FEOBV DVR within the VOI derived from this significant cluster. Figure 1.D shows that the mean ^{18}F-FEOBV DVR within that VOI was also significantly higher (9.3%; p= 0.01, t= -2.55) in the PD group (3.64 ± 0.46) compared to the control group (3.33 ± 0.26). The mean QA of the LA-tract showed no significant association.

Levodopa equivalent dose, duration or the stage of the disease did not have significant effects on the results presented above**.**

Cross-validation. Figures 2.A and 2.B show the relationship between predicted and observed values for MA-tract and VOI models, respectively. The normalized root-mean-square error was 10.36 % for the MA-tract model and 4.07 % for the VOI model, respectively, indicating a lower residual variance for the VOI model. The results of the LOO analysis mirror those of the main analysis. Figure 2.C (cf. Figure 1.C) shows a significant negative correlation between the observed mean QA (mean QA-LOO) of MA-tract and the mean ^{18}F-FEOBV DVR within the observed VOI (VOI-LOO). Figure 2.D (cf. Figure 1.D) shows that the mean ^{18}F-FEOBV DVR within VOI-LOO was significantly higher ($p= 0.04$, $t= -2.14$) in the PD group (3.58 ± 0.49) compared to the control group (3.33 ± 0.26). These findings cross-validate our observations suggesting their generalizability to independent data sets of PD subjects with similar clinical characteristics.

Association Between Dopaminergic and Cholinergic Bindings at the Presynaptic-Striatal Terminal Level in PD Subjects

^{11}C-DTBZ DVR for each of the striatal subregions and for the whole striatum showed no significant association with striatal ^{18}F-FEOBV DVR for voxel-based analysis. The same results were found after outlier removal (bilateral putaminal subregions and whole striatum in the MA hemisphere, see Supplementary Tables 1 and 2, and Supplementary Figure 1).

To further investigate the association between dopaminergic and cholinergic binding at the presynaptic terminal level, we performed post hoc correlation analysis between mean ^{18}F-FEOBV DVR within the significant cluster that correlated with mean QA in the MA hemisphere

(Figure 1. B) and the ipsilateral whole striatum^{11}C DTBZ DVR. The rationale for this post hoc analysis was that whole striatum ^{11}C DTBZ DVR and mean QA correlate with each other (Supplementary Figure 2.A). The same analysis was carried out for ^{11}C-DTBZ DVR in each striatal subregion of that hemisphere. We found that only the whole striatum ^{11}C DTBZ DVR showed a significant negative correlation (Figure 3 and Supplementary Table 3), although weaker than that observed with the mean QA (Figure 1.C). This correlation remained significant after outlier removal (Supplementary Table 3).

Striatal Cholinergic Binding in the PD Group Versus the Healthy Control Group

We found a bilateral increase in putaminal ^{18}F-FEOBV DVR in the PD group compared to the control group, more extensive in the MA hemisphere (Figure 4, Table 2). The maximum peak in each cluster was located in the posterior putamen in each hemisphere. Note the partial overlap with the findings shows in Figure 1.B. No significant decrease was found.

Clinical Correlates

Bradykinesia ratings positively correlated with our proxy measure of ACh-DA imbalance (Figure 5.A) as well as with the proxy using the measures derived from the LOO analysis (Figure 5.B). Bradykinesia ratings also negatively correlated with the mean QA of the MA-tract (Figure 5.C) and positively with the mean ^{18}F-FEOBV DVR within the putaminal VOI (Figure 5.D). The other cardinal motor features and cognitive ratings (MoCA) did not show significant associations with our proxy measure of imbalance (tremor: r= -0.08, p= 0.6; rigidity: Spearman r= 0.13, p= 0.4; Postural instability and gait difficulties: Spearman r= 0.13, p= 0.42; and MoCA: Spearman r= 0.01, p= 0.9).

Complementary findings of correlational tractography

Supplementary Figures 2.A and 2.B show the significant positive correlation found between the mean QA and the striatal ^{11}C-DTBZ DVR in both brain hemispheres, respectively. Likewise, the comparison between the two hemispheric tracts showed a significant reduction in the mean QA of the MA-tract (Supplementary Figure 2.C). The mean QA-LOO in the MA hemisphere also showed a positive correlation with the striatal ^{11}C-DTBZ DVR of that hemisphere (Supplementary Figure 2.D). The nigrostriatal dopaminergic white matter tracts followed very similar anatomical paths to those observed in our previous study (*18*).

DISCUSSION

In this study, we examined the striatal ACh-DA imbalance hypothesis in patients with early PD. Our results showed an increase in cholinergic binding in the posterior putamen of the MA brain hemisphere, associated with an ipsilateral reduction in the integrity of the nigrostriatal dopaminergic white matter tract in PD patients. In addition, cholinergic binding in this striatal region was increased in PD patients compared with normal controls. These results were cross-validated. We also showed that bradykinesia clinical sub-scores positively correlated with a proxy measure of ACh-DA imbalance in the MA hemisphere. Taken together, our results provide evidence for the striatal ACh-DA imbalance in early PD and may provide an avenue for testing in vivo effects of therapeutic strategies aimed at restoring striatal ACh-DA imbalance in PD.

Our observations are in line with previous studies in animal models of PD showing that reduced striatal dopamine signaling leads to increased excitability and synaptic reorganization of striatal cholinergic interneurons and increased acetylcholine release (for a recent review see *9*).

Our findings suggest that the association between acetylcholine (^{18}F-FEOBV binding) and the integrity loss of the nigrostriatal dopaminergic pathway is stronger and more robust at the level of dopaminergic nigrostriatal connectivity (i.e., loss of mean QA of the nigrostriatal tract, Figure 1.C) compared to the presynaptic-terminal level (i.e., loss of striatal ^{11}C-DTBZ binding, Figure 3). This finding is probably due to several factors: first, ^{11}C-DTBZ binding may underestimate damage severity to the nigrostriatal end-terminal in PD due to compensatory changes (*17*). In contrast, the mean QA of the most affected hemispheric tract fibers is probably less influenced by the ^{11}C-DTBZ's compensation mechanism. The estimation of the mean QA not only uses the information derived from the ^{11}C-DTBZ PET but also white matter fibers derived from dMRI. Second, striatal neurotransmission involves not only acetylcholine and dopamine but also other extrinsic (e.g., glutamatergic projections from the thalamus and cortex) and intrinsic determinants (e.g., GABAergic interneurons), which may have interacting effects with striatal dopaminergic neurons and cholinergic interneurons at the level of presynaptic nerve terminals (for recent reviews see *7*-*9*). In contrast, the dopaminergic nigrostriatal tract includes structural connectivity information specific for dopaminergic neurotransmission and thus less affected by other neurotransmitter interactions. It is also possible that cholinergic upregulation may be more prominent in the prodromal stage but becomes less in the symptomatic stage of PD, thus diluting the possible one-to-one relationship between striatal acetylcholine and dopamine at the level of presynaptic nerve terminals (*36*). Therefore, the dopaminergic nigrostriatal tract may be a more precise marker of the integrity of the nigral dopaminergic cells compared to the more downstream distal degeneration of the nerve terminals. The observed decrease in the tract integrity could be the result of the distal-to-proximal axonal degenerative “back-dying” process in PD (*37*).

Our proxy measure for ACh-DA imbalance was positively correlated with clinical bradykinesia ratings. This finding may be explained by the fact that bradykinesia has the closest association with striatal dopaminergic activity compared to the other cardinal motor symptoms (*38*). This observation also agrees with a previous study in a PD mouse model showing that photoinhibition of striatal cholinergic interneurons reduces bradykinesia (*39*). Other cardinal symptoms and cognitive function did not show an association with our imbalance proxy. These other impairments are likely caused by more expanded brain networks that extend beyond the striatum (*40-42*). Our study focused only on the striatum to reduce the complexity of the ACh-DA interactions and to make it also consistent with the existing literature on the ACh-DA imbalance in PD.

The discrepant findings between some previous animal studies (*10-12*) and our current in vivo human PD results may be related to differences between the generally more uniform toxic or lesioning animal PD models versus the natural history of the insidious and long duration of dopaminergic degeneration, and interindividual variability in patients with PD. Moreover, our presynaptic vesicular transporter PET measures may reflect a more relative "steady state" of the integrity of nerve terminals rather than the typical more dynamic signaling changes observed in animal models.

A strength of this study is the use of ^{11}C-DTBZ PET-informed correlational tractography (*18*). We also replicated and extended this methodology in a larger sample of patients with early PD. Unlike our previous study, we were able to also cross-validate the tract in the MA hemisphere probably due to the larger sample that allowed a more robust estimate of the "tract template" in that hemisphere.

Our study has several limitations. First, dopaminergic PET was performed in the dopaminergic medication "OFF" state whereas cholinergic PET was performed on dopaminergic medications. Nevertheless, it is possible that the imbalance between the acetylcholine and dopamine markers would have been even greater than that observed in this study if both PET scans had been performed in the "OFF" state. Second, our study was cross-sectional precluding us to evaluate the evolution of the ACh-DA interaction in PD over time. Third, the effect of gender or clinical phenotype on the ACh-DA interaction was not assessed as larger samples of PD subjects would be needed for this purpose. Fourth, we were unable to investigate the ACh-DA interaction in normal controls due to the lack of ^{11}C-DTBZ PET in these subjects. However, a lower putaminal ^{18}F-FEOBV DVR found in normal controls compared with PD patients may be consistent with the prevailing view is that acetylcholine and dopamine are balanced in healthy conditions. Other limitations are related to the methodology to estimate the nigrostriatal dopaminergic tracts (*18*). For example, we cannot rule out that the identified tracts also include some non-dopaminergic fibers; and the identified tracts extended slightly below the substantia nigra, which may be due to limitations in the spatial resolution of dMRI. Nonetheless, the use of ^{11}C-DTBZ PET-informed correlational tractography has higher dopaminergic specificity compared to tract definition using dMRI alone. Finally, future neuroimaging studies should take into account more expanded brain networks and other key players that could shed more light on the complexity of ACh-DA interaction (e.g., dopaminergic and cholinergic receptors as well as other neurotransmitters).

CONCLUSION

Using dual-tracer PET and dopaminergic PET-informed correlational tractography, we provided in vivo evidence of imbalance between acetylcholine and dopamine signaling systems

in the striatum in early PD. These observations may provide a future avenue for testing in vivo effects of therapeutic strategies aimed at restoring striatal ACh-DA imbalance in PD.

DISCLOSURE:

Nothing to disclose.

ACKNOWLEDGMENTS

We thank Christine Minderovic, Cyrus Sarosh, Jacqueline Dobson, PET technologists, cyclotron operators, and radiochemists. We also thank funding agencies: the NIH, the Department of Veterans Affairs, and the Michael J. Fox Foundation. Special thanks to our patients with PD and research volunteers.

KEY POINTS

QUESTION: Is there an imbalance between the acetylcholine and dopamine signaling systems in the striatum in early PD?

PERTINENT FINDINGS: In a cohort study, using cholinergic and dopaminergic PET and correlational tractography, an imbalance was found between the acetylcholine and dopamine signaling systems in the striatum in 45 patients with mild to moderate PD. This imbalance was evidenced by an increase in cholinergic binding in the posterior putamen in the most affected brain hemisphere that correlated with the ipsilateral reduction in the integrity of the dopaminergic nigrostriatal white matter tract and clinically with more severe bradykinesia.

IMPLICATIONS FOR PATIENT CARE: Assessment of the striatal acetylcholine-dopamine imbalance may provide a method for in vivo testing the effects of therapeutic strategies aimed at reducing this imbalance in early PD.

REFERENCES

1. Mesulam MM, Mash D, Hersh L, Bothwell M, Geula C. Cholinergic innervation of the human striatum, globus pallidus, subthalamic nucleus, substantia nigra, and red nucleus. *J Comp Neurol*. 1992;323:252–268.
2. Bolam JP, Wainer BH, Smith AD. Characterization of cholinergic neurons in the rat neostriatum. A combination of choline acetyltransferase immunocytochemistry, Golgi-impregnation and electron microscopy. *Neuroscience.* 1984;12:711–8.
3. Barbeau A. The pathogenesis of Parkinson's disease: a new hypothesis. *Can Med Assoc J.* 1962;87:802–807.
4. Aosaki T, Miura M, Suzuki T, Nishimura K, Masuda M. Acetylcholine-dopamine balance hypothesis in the striatum: an update. *Geriatr Gerontol Int*. 2010;10 Suppl 1:S148-57.
5. Lang AE, Lozano AM. Parkinson's disease: second of two parts. *N Engl J Med*. 1998; 339:1130–1143.
6. Bridi JC, Hirth F. Mechanisms of a-synuclein induced synaptopathy in Parkinson's disease. *Front Neurosci*. 2018;12:80.
7. Girasole AE, Nelson AB. Probing striatal microcircuitry to understand the functional role of cholinergic interneurons. *Mov. Disord*. 2018;30:1306–1318.
8. Tanimura A, Pancani T, Lim SAO, et al. Striatal cholinergic interneurons and Parkinson's disease. *Eur. J. Neurosci*. 2018;47:1148-1158.
9. Ztaou S, Amalric M. Contribution of cholinergic interneurons to striatal pathophysiology in Parkinson's disease. *Neurochem Int*. 2019;126:1–10.

10. Herrera-Marschitz M, Goiny M, Utsumi H, et al. Effect of unilateral nucleus basalis lesion on cortical and striatal acetylcholine and dopamine release monitored in vivo with microdialysis. *Neurosci Lett*.1990;110:172–9.
11. Herrera-Marschitz M, Luthman J, Ferre S. Unilateral neonatal intracerebroventricular 6-hydroxydopamine administration in rats: II. Effects on extracellular monoamine, acetylcholine and adenosine levels monitored with in vivo microdialysis. *Psychopharmacology (Berl).* 1994;116:451–456.
12. McKinley JW, Shi ZQ, Kawikova I, et al. Dopamine deficiency reduces striatal cholinergic interneuron function in models of Parkinson's disease. *Neuron*. 2019;103:1056–1072.
13. Petrou M, Frey KA, Kilbourn MR, et al. In vivo imaging of human cholinergic nerve terminals with (-)-5-^{18}F-fluoroethoxybenzovesamicol: biodistribution, dosimetry, and tracer kinetic analyses. *J Nucl Med*. 2014;55:396-404.
14. Bohnen NI, Albin RL, Koeppe RA, et al. Positron emission tomography of monoaminergic vesicular binding in aging and Parkinson disease. *J Cereb Blood Flow Metab*. 2006;26:1198–1212.
15. Perlmutter JS, Norris SA. Neuroimaging biomarkers for Parkinson disease: facts and fantasy. *Ann Neurol*. 2014;76:769-783.
16. de la Fuente-Fernández R. Imaging of Dopamine in PD and Implications for Motor and Neuropsychiatric Manifestations of PD. *Front Neurol*. 2013;4:90.
17. de la Fuente-Fernández R, Sossi V, McCormick S, Schulzer M, Ruth TJ, Stoessl AJ. Visualizing vesicular dopamine dynamics in Parkinson's disease. *Synapse*. 2009;63:713-6.
18. Sanchez-Catasus CA, Bohnen NI, Yeh FC, D'Cruz N, Kanel P, Müller M L T M. Dopaminergic nigrostriatal connectivity in early Parkinson disease: in vivo neuroimaging

study of 11 C-DTBZ PET combined with correlational tractography. *J Nucl Med*. 2021;62: 545:552.

19. Yeh FC, Tseng WY. NTU-90: a high angular resolution brain atlas constructed by q-space diffeomorphic reconstruction. *Neuroimage*. 2011;58:91–99.
20. Zhang H, Wang Y, Lu T, et al. Differences between generalized q-sampling imaging and diffusion tensor imaging in the preoperative visualization of the nerve fiber tracts within peritumoral edema in brain. *Neurosurgery*. 2013;73:1044–1053.
21. Yeh FC, Vettel JM, Singh A, et al. Quantifying differences and similarities in whole-brain white matter architecture using local connectome fingerprints. *PLOS Comput Biol.* 2016;12:e1005203.
22. Hughes AJ, Daniel SE, Kilford L, Lees AJ. Accuracy of clinical diagnosis of idiopathic Parkinson's disease: a clinico-pathological study of 100 cases. *J Neurol Neurosurg Psychiatry*.1992;55:181–184.
23. Goetz CG, Fahn S, Martinez-Martin P, et al. Movement Disorder Society-sponsored revision of the Unified Parkinson's Disease Rating Scale (MDS-UPDRS): process, format, and clinimetric testing plan. *Mov Disord*.2007;22:41-47.
24. Hoehn MM, Yahr MD. Parkinsonism: onset, progression and mortality. *Neurology*. 1967;17:427-442.
25. Nasreddine ZS, Phillips NA, Bedirian V, et al. The Montreal Cognitive Assessment, MoCA: a brief screening tool for mild cognitive impairment. *J Am Geriatr Soc*.2005;53:695-9.
26. Müller ML, Albin RL, Kotagal V, et al. Thalamic cholinergic innervation and postural sensory integration function in Parkinson's disease. *Brain*. 2013;136:3282–3289.

27. Bohnen NI, Kanel P, Zhou Z, et al. Cholinergic system changes of falls and freezing of gait in Parkinson disease. *Ann Neurol*. 2019;85:538-549.

28. Jewett DM, Kilbourn MR, Lee LC. A simple synthesis of [11C] dihydrotetrabenazine (DTBZ). *Nucl Med Biol.*1997;24:197–199.

29. Shao X, Hoareau R, Hockley BG, et al. Highlighting the Versatility of the Tracerlab Synthesis Modules. Part 1: Fully Automated Production of [F]Labelled Radiopharmaceuticals using a Tracerlab FX(FN). J Labelled Comp Radiopharm. 2011;54:292-307.

30. Minoshima S, Frey KA, Koeppe RA, Foster NL, Kuhl DE. A diagnostic approach in Alzheimer's disease using three-dimensional stereotactic surface projections of fluorine-18-FDG PET. *J Nucl Med*. 1995;36:1238–1248.

31. Logan J, Fowler JS, Volkow ND, Wang GJ, Ding YS, Alexoff DL. Distribution volume ratios without blood sampling from graphical analysis of PET data. *J Cereb Blood Flow Metab*. 1996;16:834–840.

32. Nejad-Davarani S, Koeppe RA, Albin RL, Frey KA, Muller M, Bohnen NI. Quantification of brain cholinergic denervation in dementia with Lewy bodies using PET imaging with [(^{18})F]-FEOBV. *Mol Psychiatry*. 2019;24:322-327.

33. Kwak Y, Bohnen NI, Müller MLTM, Dayalu P, Seidler RD. Striatal denervation pattern predicts levodopa effects on sequence learning in Parkinson's disease. *J Mot Behav.* 2013;45:423–429.

34. Yeh FC, Wedeen VJ, Tseng WY. Generalized q-sampling imaging. *IEEE Trans Med Imaging*. 2010;29:1626–1635.

35. Yeh FC, Verstynen TD, Wang Y, Fernández-Miranda JC, Tseng WY. Deterministic diffusion fiber tracking improved by quantitative anisotropy. *PLoS One.* 2013;8:e80713.
36. Liu S-Y, Wile DJ, Fu J, et al. The influence of LRRK2 mutations on the cholinergic system in manifest and prodromal stages of Parkinson's disease: a cross-sectional PET study. *Lancet Neurol*. 2018;17:309-316.
37. Tagliaferro P, Burke RE. Retrograde Axonal Degeneration in Parkinson Disease. *J Parkinsons Dis*. 2016;6:1-15.
38. Vingerhoets FJ, Schulzer M, Calne DB, Snow BJ. Which clinical sign of Parkinson's disease best reflects the nigrostriatal lesion? *Ann Neurol*. 1997;41:58-64.
39. Ztaou S, Maurice N, Camon J, et al. Involvement of Striatal Cholinergic Interneurons and M1 and M4 Muscarinic Receptors in Motor Symptoms of Parkinson's Disease. *J Neurosci.* 2016;36:9161-9172.
40. Dirkx MF, den Ouden H, Aarts E, et al. The Cerebral Network of Parkinson's Tremor: An Effective Connectivity fMRI Study. *J Neurosci*. 2016;36:5362-5372.
41. Baradaran N, Tan SN, Liu A, et al. Parkinson's disease rigidity: relation to brain connectivity and motor performance. *Front Neurol*. 2013;4:67.
42. Kehagia AA, Barker RA, Robbins TW. Cognitive impairment in Parkinson's disease: the dual syndrome hypothesis. *Neurodegener Dis*. 2013;11:79-92.

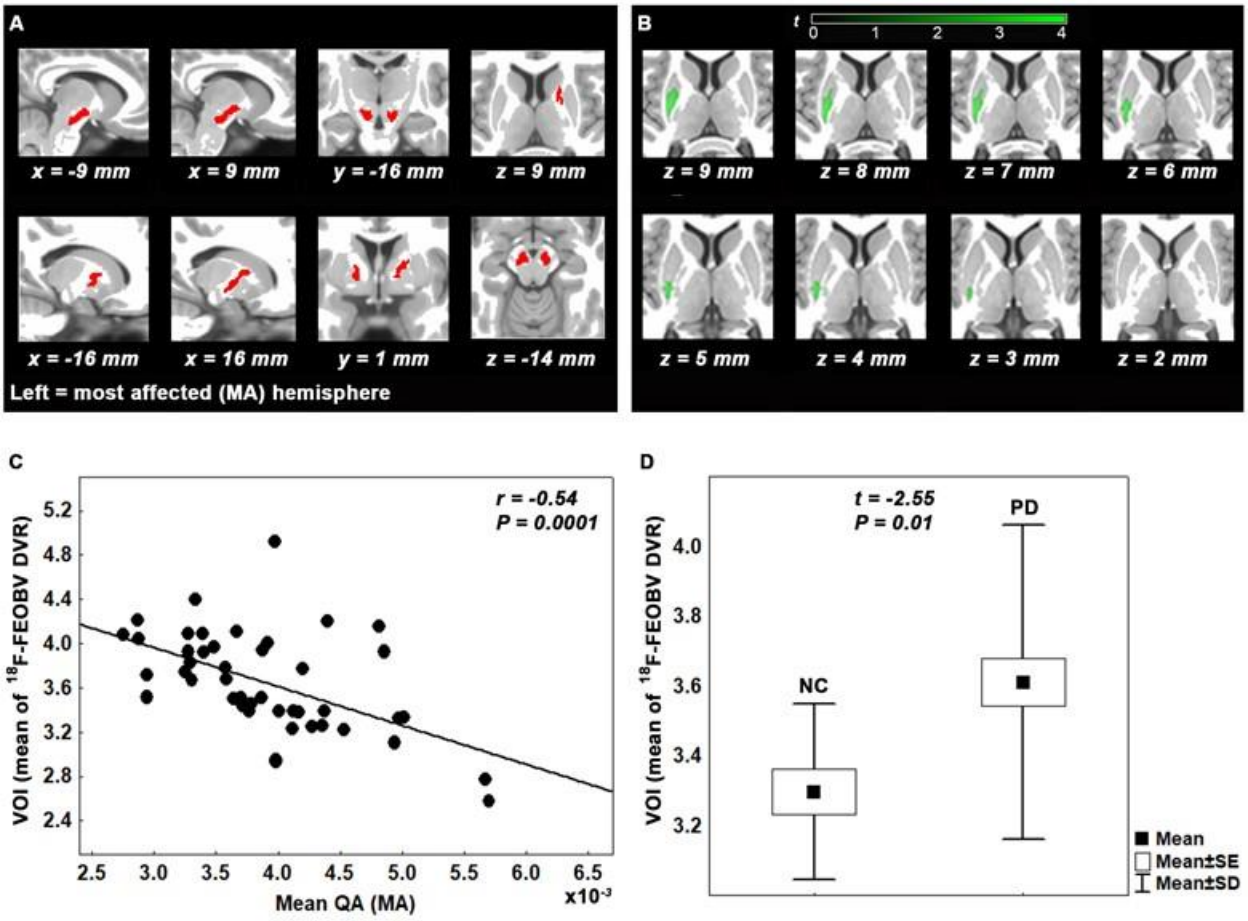

Figure. 1. (A) Nigrostriatal dopaminergic white matter tracts identified in the PD group in the most (MA) and least affected (LA) hemispheres (overlaid on a T1-weighted MR image in MNI space). (B) Voxel-based correlation analysis showing a negative correlation between the mean QA of the MA tract with ^{18}F-FEOBV DVR in the posterior putamen of the same hemisphere. (C) Negative correlation between the mean QA of the MA tract and the mean ^{18}F-FEOBV DVR within the putaminal SPM-based VOI (95 % CI: -0.76, -0.2). (D) The mean ^{18}F-FEOBV DVR within that putaminal VOI was significantly higher in the PD group compared to the normal control (NC) group.

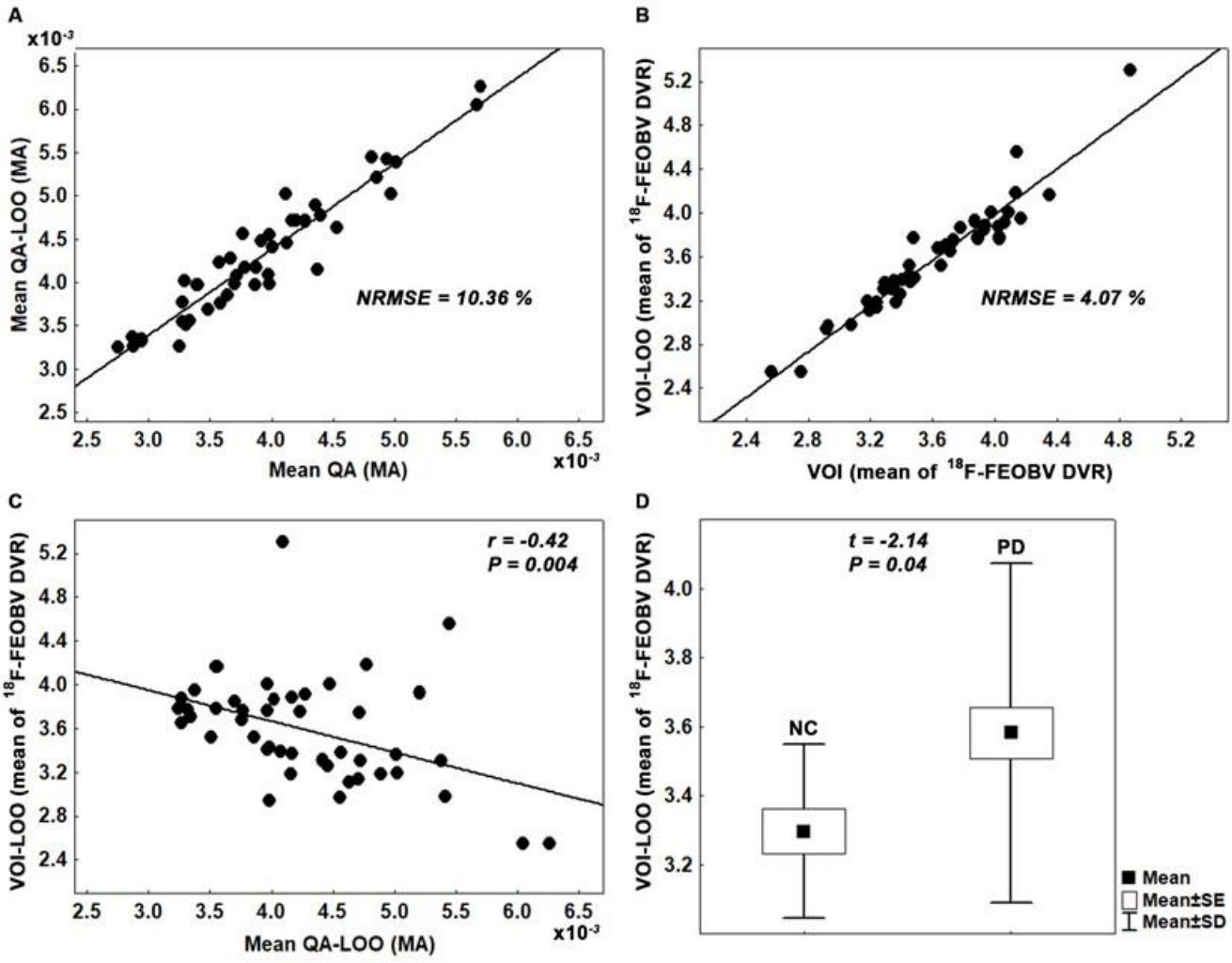

Figure. 2. (A) Relation between training (predicted values) and cross-validation (observed values) sets using leave-one-out (LOO) approach (mean QA and mean QA-LOO, respectively) in the MA hemisphere of PD subjects. (B) Same as shown in (A) but for the VOI model derived from the SPM voxel-based correlation analysis (VOI and VOI-LOO, respectively). (C) Negative correlation between the mean QA-LOO of the MA tract and the mean ^{18}F-FEOBV DVR within the VOI-LOO (95 % CI: -0.75, -0.09). (D) The mean ^{18}F-FEOBV DVR within the VOI-LOO was also significantly higher in the PD group compared to the normal control (NC) group.

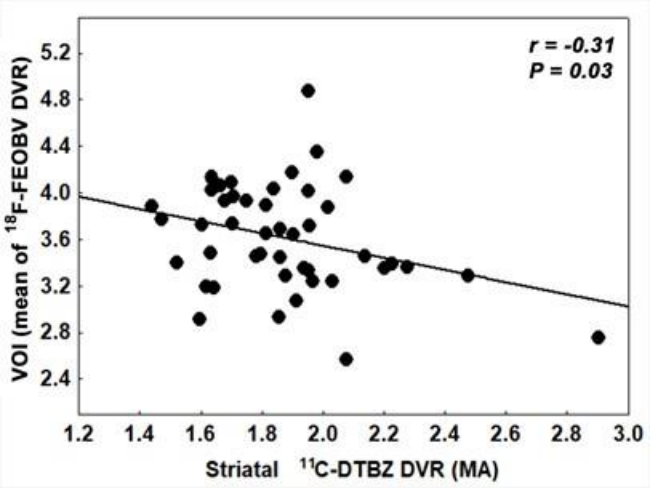

Figure. 3. Negative correlation between mean ^{18}F-FEOBV DVR within the significant cluster correlated with mean QA in the MA hemisphere (Figure 1. B) and the ipsilateral whole striatum^{11}C DTBZ DVR (95 % CI: -0.55, -0.02).

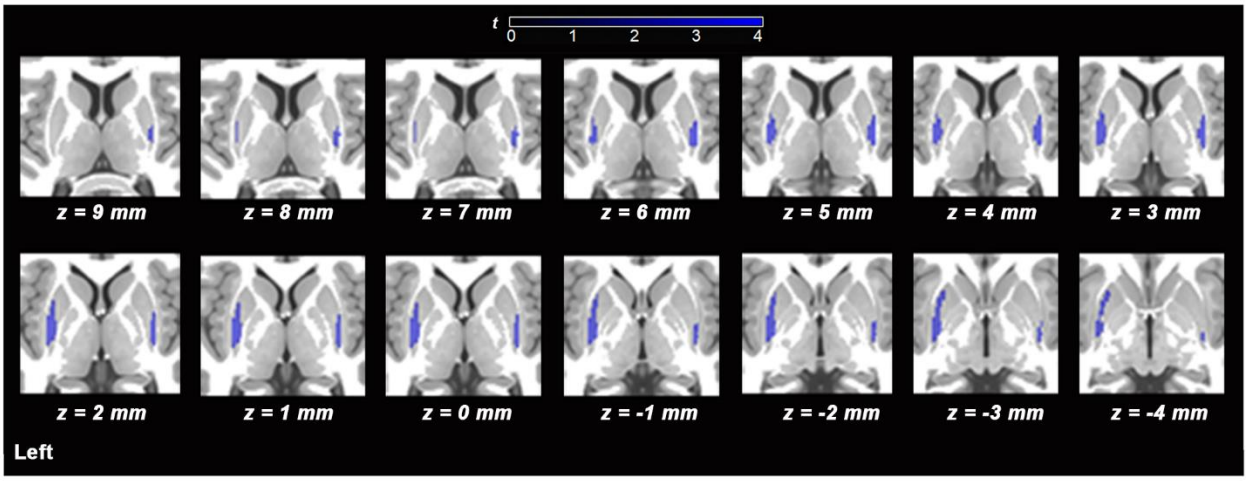

Figure. 4. Voxel-based group comparison analysis showing asymmetric bilateral putaminal ^{18}F-FEOBV DVR increases (more extensive in the MA hemisphere, left side in the Figure) compared to the control group (see also Table 2). Note the partial topographic overlap of the MA side with the results of the voxel-based correlation analysis in the PD group (cf. Figure. 1.B, z = 6 to 4 mm, left side).

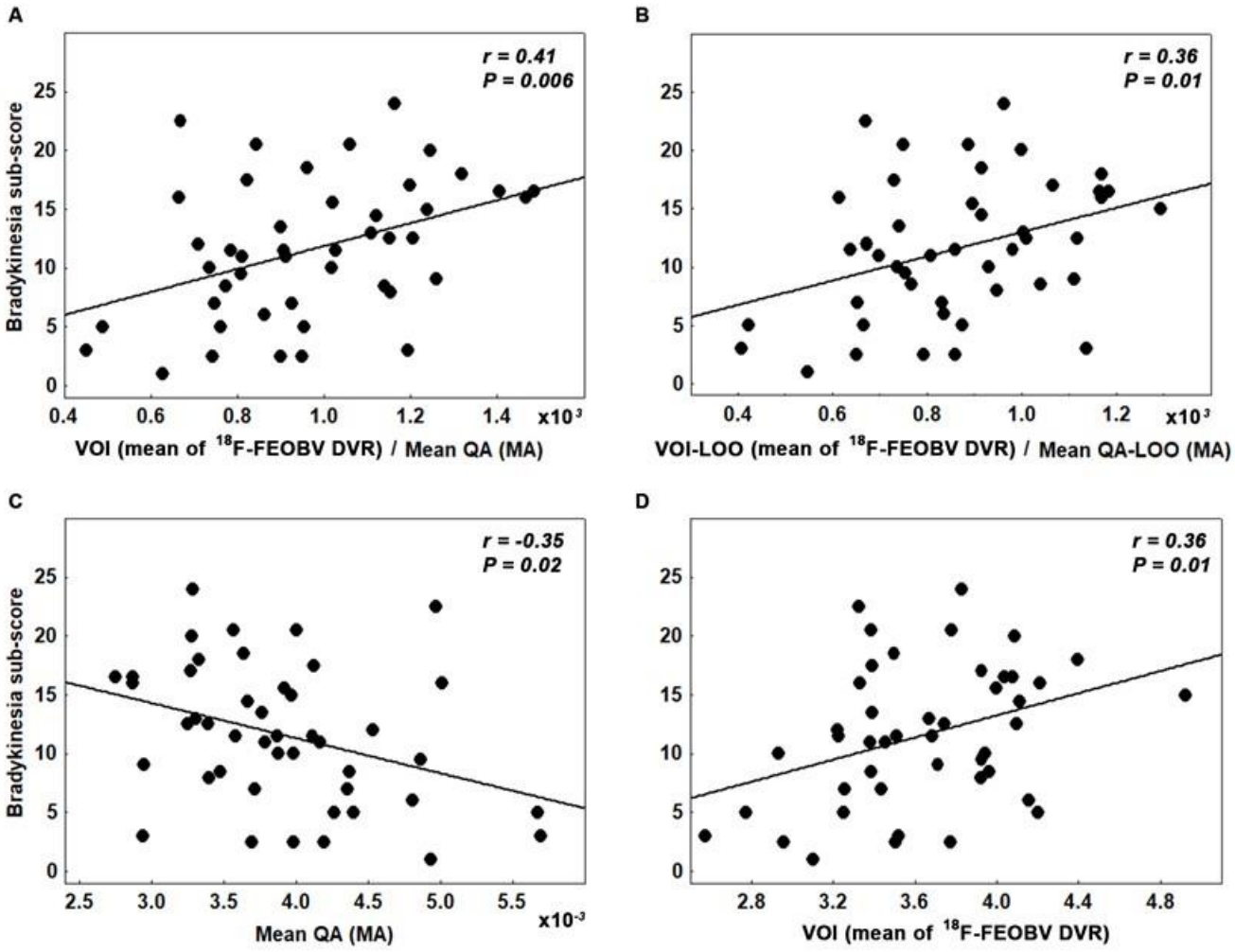

Figure. 5. (A) A positive correlation between the bradykinesia sub-score and a proxy measure of acetylcholine-dopamine imbalance in the MA hemisphere in subjects with PD (95 % CI: 0.15, 0.62). **(B)** Same as shown in (A) but using the measures derived from the leave-one-out (LOO) cross-validation analysis (95 % CI: 0.07, 0.59). **(C)** Negative correlation between the bradykinesia sub-score and mean QA in the MA hemisphere (95 % CI: -0.63, -0.01). **(D)** Positive correlation between the bradykinesia sub-score and the mean ^{18}F-FEOBV DVR within the putaminal SPM-based VOI in the MA hemisphere (95 % CI: 0.1, 0.58).

TABLES

Table 1. Demographic and clinical characteristics of PD and control subjects.

	PD (n = 45)	Control (n = 15)	Statistical significance
Age (years)	66.3 ± 6.3	69.1 ± 8.6	t = 1.3 ; p = 0.19
Sex (males/females)	36/9	9/6	$\chi 2 = 2.4$; p = 0.12
Handedness (right/left)	41/4	13/2	$\chi 2 = 0.25$; p = 0.62
MoCA	27.0 ± 2.6	27.6 ± 1.8	t = 0.87 ; p = 0.39
MDS-UPDRS (part I)	5.1 ± 4.5		
MDS-UPDRS (part II)	5.5 ± 3.5		
MDS-UPDRS (part III)	34.3 ± 13.2		
Bradykinesia sub-score*	11.6 ± 5.9		
Tremor sub-score*	8.8 ± 4.4		
Rigidity sub-score*	7.5 ± 2.9		
PIGD sub-sccore*	2.5 ± 2		
MDS-UPDRS (I -III) total score	44.9 ± 16.8		
Hoehn and Yahr stage	2.2 ± 0.6 (2,5; 1-3) †		
Disease duration (years)	5.8 ± 3.6		
Levodopa equivalent dose (mg)	636.6 ± 374.5		

MoCA = Montreal Cognitive Assessment. MDS-UPDRS = Movement Disorder Society-revised Unified Parkinson's Disease Rating Scale. PIGD = Postural Instability and Gait Difficulties. *****derived from MDS-UPDRS (part III). †In brackets, median; minimum –maximum of Hoehn and Yahr stage.

Table 2. Striatal cholinergic bidding increase in the PD group compared to the control group.

Striatal region	$P_{FWE\text{-}corr}$ Cluster-level	Cluster size	MNI coordinates (x, y, z) of the maximum peak	Peak-level *t* value
MA* Putamen	0.028	369 voxels	-32, -8, 5	3.93
LA† Putamen	0.043	188 voxels	32, -9, 6	4.15

MA* (LA†) = clinically most (least) affected hemisphere in PD patients.

GRAPHICAL ABSTRACT

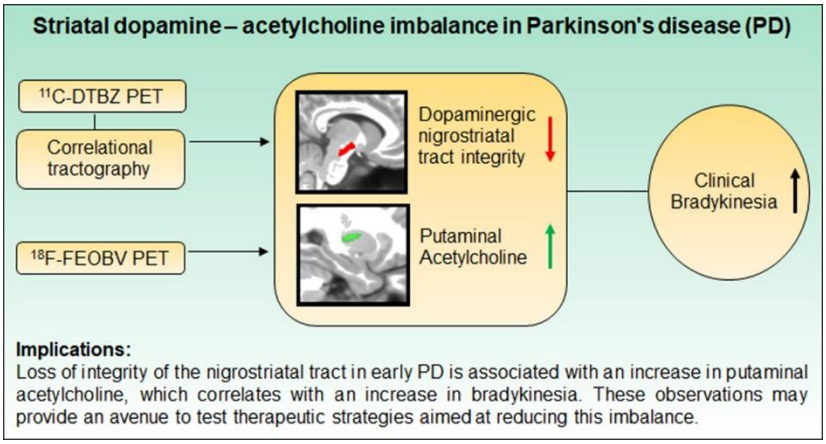

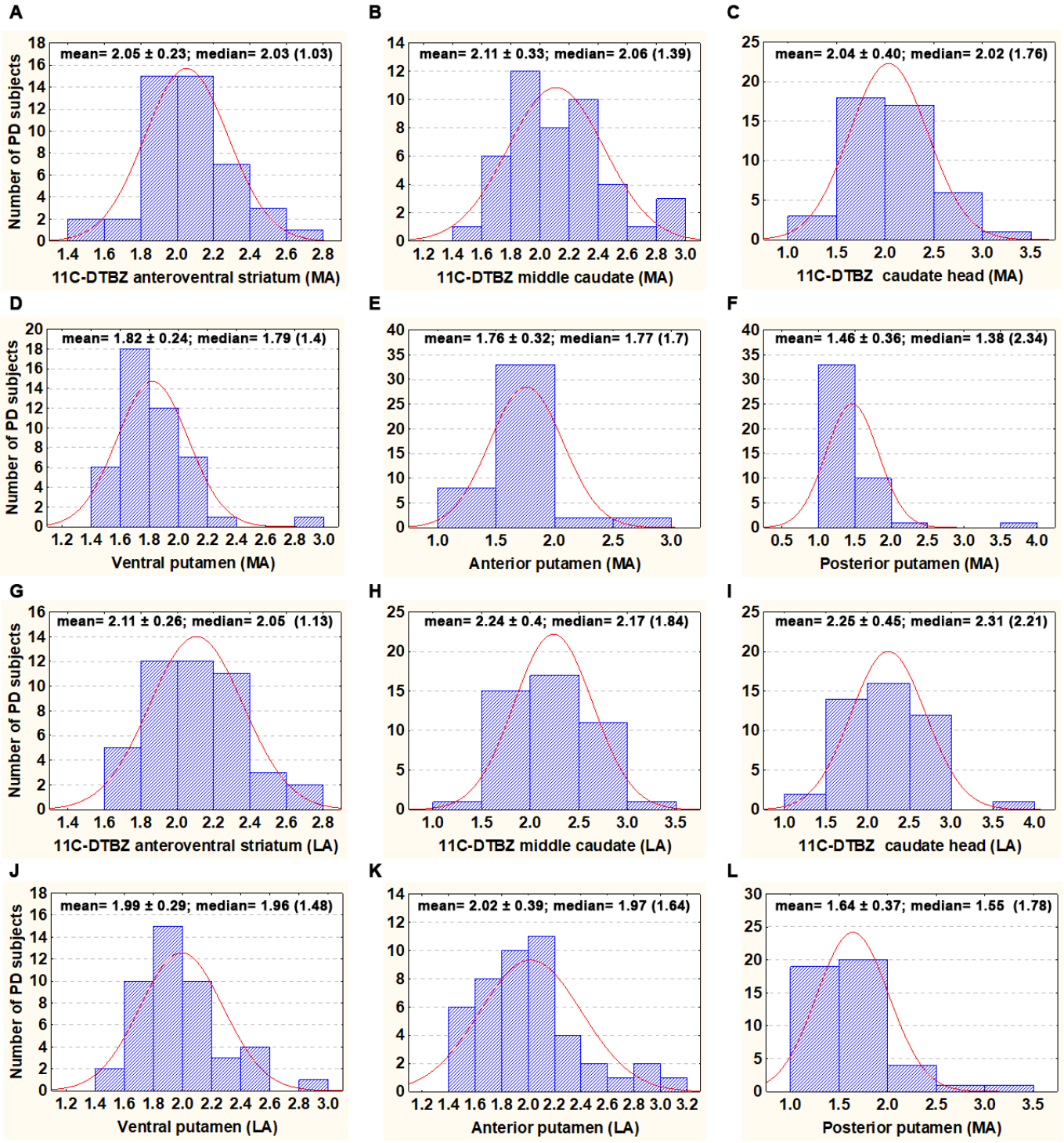

Supplementary Figure 1. Histograms, mean (± standard deviation), and median (range) of ^{11}C-DTBZ DVR in six striatal subregions, whole striatum and mean QA in each brain hemisphere in the participants with early PD (N=45). MA (LA) = clinically most (least) affected hemisphere.

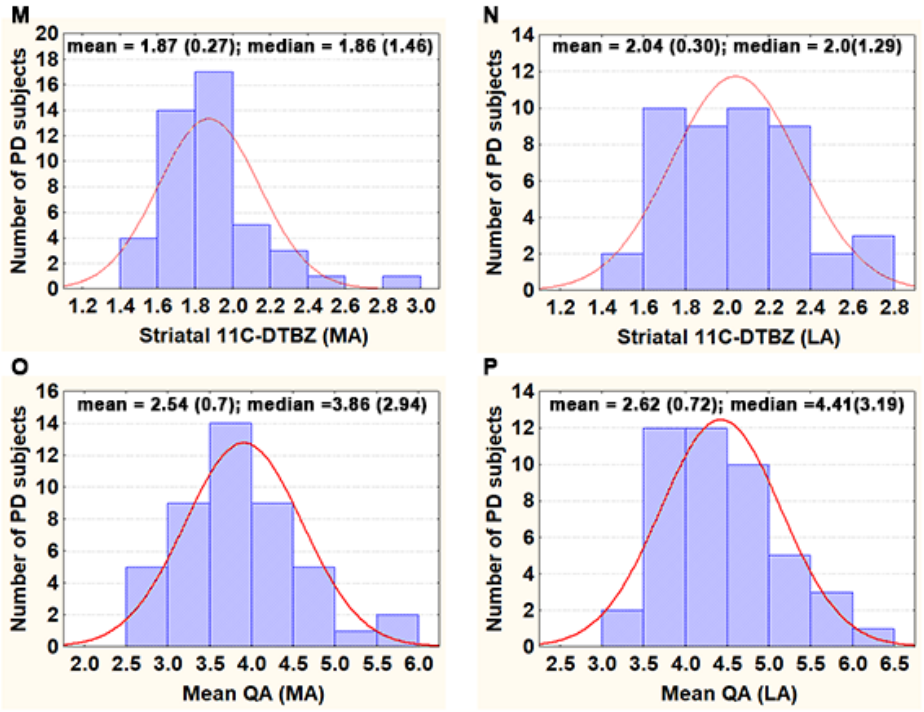

Supplementary Figure 1. (continuation from the previous page).

Supplementary Table 1. Results of the normality tests (Shapiro-Wilk zW test) and the detection of outliers (Grubbs test) in ^{11}C-DTBZ DVR of striatal subregions, whole striatum and mean QA in both hemispheres.

Subregion	Shapiro-Wilk W	p-value	Grubbs Test	p-value
AVS (MA*)	0.97	0.26	2.40	1.0
Middle Caudate (MA)	0.98	0.47	2.24	1.0
Caudate head (MA)	0.98	0.76	2.45	1.0
Ventral putamen (MA)	0.83	10^{-5}	4.50	$1.7x10^{-5}$
Anterior putamen (MA)	0.85	$4x10^{-5}$	3.90	0.001
Posterior putamen (MA)	0.51	$> 10^{-6}$	5.76	$> 10^{-6}$
Whole striatum (MA)	0.95	0.06	3.20	0.04
AVS (LA†)	0.96	0.17	2.63	0.57
Middle Caudate (LA)	0.98	0.65	2.62	0.58
Caudate head (LA)	0.98	0.60	2.85	0.26
Ventral putamen (LA)	0.93	0.02	3.49	0.015
Anterior putamen (LA)	0.94	0.02	3.20	0.04
Posterior putamen (LA)	0.80	10^{-6}	3.71	0.0047
Whole striatum (LA)	0.97	0.30	2.42	1.0
Mean QA (MA)	0.96	0.11	2.55	0.76
Mean QA (LA)	0.96	0.19	2.62	0.59

QA= quantitative anisotropy. AVS = anteroventral striatum. MA* (LA†) = clinically most (least) affected hemisphere in PD patients.

Supplementary Table 2. Results of the interquartile rule to find outliers in ^{11}C-DTBZ DVR of subregions significant for the Grubbs test as shown in Supplementary Table 1.

Putaminal subregion	Interquartile range	Lower boundary	Upper boundary	Number of potential outliers
Ventral putamen (MA*)	0.23	1.34	2.24	2 upper
Anterior putamen (MA)	0.34	1.06	2.40	2 upper
Posterior putamen (MA)	0.20	1.00	1.81	2 upper
Whole striatum (MA)	0.29	1.25	2.48	1 upper
Ventral putamen (LA†)	0.33	1.30	2.61	1 upper
Anterior putamen (LA)	0.45	1.08	2.86	2 upper
Posterior putamen (LA)	0.32	0.94	2.23	4 upper

MA* (LA†) = clinically most (least) affected hemisphere in PD patients.

Supplementary Table 3. Correlation between the mean DVR within the significant ^{18}F-FEOBV cluster in the MA hemisphere (Figure 1. B in the main text) and ^{11}C-DTBZ DVR in striatal subregions and whole striatum of that hemisphere (post hoc analysis).

Striatal subregions	Pearson	Pearson*	Spearman**	Spearman***
AVS	-0.27 *(0.07);* -0.52, -0.03	-	-	-
Middle Caudate	-0.20 *(0.17);* -0.48, -0.09	-	-	-
Caudate head	-0.20 *(0.18);* -0.45, -0.07	-	-	-
Ventral putamen	-0.33 *(0.03);* -0.57, -0.04	-0.17 *(0.3);* -0.42, 0.13	-0.29 *(0.05);* -0.51, -0.05	-0.26 (*0.09*); -0.47, 0.03
Anterior putamen	-0.30 *(0.04);* -0.55, -0.01	-0.13 *(0.4);* -0.41, 0.17	-0.26 *(0.08);* -0.48, 0.02	-0.24 (*0.11*); -0.46, 0.01
Posterior putamen	-0.34 *(0.02);* -0.58, -0.05	-0.17 *(0.3);* *-0.43, 0.12*	-0.23 *(0.13);* -0.45, 0.02	-0.21 (*0.17*); -0.45, 0.02
Whole striatum	-0.31 *(0.03);* -0.55, -0.02	-0.31 *(0.04);* -0.55, -0.01	-	-

*Pearson correlation coefficients after outlier removal in the variables that had this behavior (see Supplementary Table 2). ** Spearman correlation coefficients for non-normal distributed variables (see Supplementary Figure 1). ***Spearman correlation after outlier removal. The p-value appears *in italics* (*in parentheses*) to the right of each correlation coefficient; lower and upper confidence intervals appear after a semicolon.

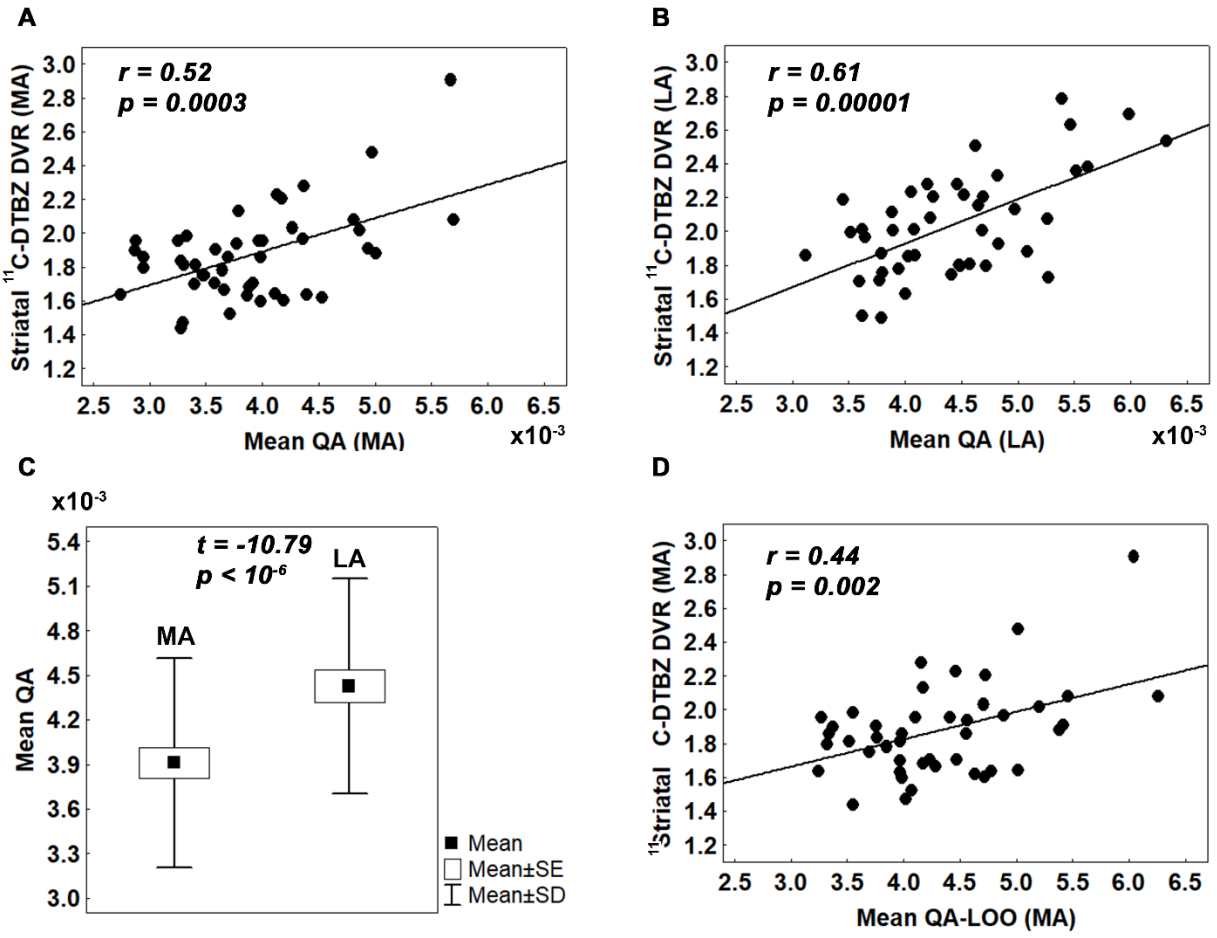

Supplementary Figure 2. (A) Mean QA of the MA nigrostriatal white matter tract positively correlates with whole striatum ^{11}C–DTBZ DVR values in the MA hemisphere (95 % CI: 0.21- 0.69 (B) The same as (B) for the LA tract (95 % CI: 0.35 - 0.76). (C) Comparison between the two tracts shows a significant reduction in the mean QA of the MA tract (3.91 ± 0.70 x 10^{-3}) compared to the LA tract (4.43 ± 0.72 x 10^{-3}). (D) Leave One Out (LOO) analysis of the nigrostriatal white matter tract in the MA hemisphere. Mean QA-LOO (MA) showed a positive correlation with whole striatum ^{11}C–DTBZ DVR values in the MA hemisphere (95 % CI: 0.15- 0.63).